Preprints.org

Article

Not peer-reviewed version

New Structures of Synchronous Motor with Two Stators and Single Rotor, with High-Energy NdFeB Permanent Magnets Arranged on Both Rotor Bores

Mihail-Florin Stan *, Iulian Bancuta, Traian Ivanovici

Posted Date: 4 August 2025

doi: 10.20944/preprints202508.0088.v1

Keywords: NdFeB permanent magnets; double stator; electromagnetic performance; double active surfaces

Preprints.org is a free multidisciplinary platform providing preprint service that is dedicated to making early versions of research outputs permanently available and citable. Preprints posted at Preprints.org appear in Web of Science, Crossref, Google Scholar, Scilit, Europe PMC.

Copyright: This open access article is published under a Creative Commons CC BY 4.0 license, which permit the free download, distribution, and reuse, provided that the author and preprint are cited in any reuse.

Preprints.org (www.preprints.org) | NOT PEER-REVIEWED | Posted: 4 August 2025 doi:10.20944/preprints202508.0088.v1

Disclaimer/Publisher's Note: The statements, opinions, and data contained in all publications are solely those of the individual author(s) and contributor(s) and not of MDPI and/or the editor(s). MDPI and/or the editor(s) disclaim responsibility for any injury to people or property resulting from any ideas, methods, instructions, or products referred to in the content.

Article

New Structures of Synchronous Motor with Two Stators and Single Rotor, with High-Energy NdFeB Permanent Magnets Arranged on Both Rotor Bores

Mihail-Florin Stan [1,*], Iulian Bancuta [1] and Traian Ivanovici [2]

[1] Department of Automatics, Informatics, and Electrical Engineering, Valahia University of Targoviste, 130004 Targoviste, Romania

[2] Department of Electronics, Telecommunications and Power Engineering, Valahia University of Targoviste, 130004 Targoviste, Romania

* Correspondence: florin.stan@valahia.ro or flo.stan@gmail.com

Abstract

The first permanent magnet electric machines appeared in the first half of the last century and their evolution was continuous as magnets with high magnetic energies appeared and magnetic circuits were created that allowed for efficient use of the magnets. The solution of the asynchronous motor with two stators with a massive rotor described in previous work opened the way to a synchronous variant of the machine with two stators, using rare earth permanent magnets, which are arranged on both cylindrical surfaces of the rotor. In this way, the volume of the magnets and the flux of the machine can be increased. The rotor construction made of solid steel, mechanically robust, does not disturb from an electromagnetic point of view, because it rotates synchronously with the fundamental of the stator field, so it will no longer induce eddy currents in the rotor iron in a permanent regime. In the synchronous variant, part of the inductor flux is closed through the rotor, which can be an advantage for the optimal use of the active surfaces of the machine.

Keywords: NdFeB permanent magnets; double stator; electromagnetic performance; double active surfaces

1. Introduction

The greatest developments in the field of permanent magnet integration have been achieved in the last 20 years, with the intensive use of rare earth magnets, especially after the discovery of the NdFeB alloy [1–5], which has the highest magnetic energy.

In the field of synchronous machines, permanent magnets have been used to replace electromagnetic excitation. The advantages that arise from this are the following: simplification of construction by eliminating excitation windings, the absence of any sliding contacts, greater operational reliability, reduced overall dimensions and higher efficiency due to the elimination of excitation losses [6–10].

If in the construction of generators the use of magnets is limited, due to the impossibility of regulating the excitation flux, synchronous motors with permanent magnets are widely used, in numerous constructive variants. By properly calculating the magnetic circuit, it is possible to operate at unit or even capacitive power factor, a fact unachievable in another type of motor **[11]**. The lack of sliding contacts, therefore of sparks, recommends these motors in drives intended to work in explosive environments. Powered by static frequency converters, synchronous motors with permanent magnets are used in applications where good speed regulation within wide limits is required [12–15]. A decisive advantage is the property of these motors to maintain their speed unchanged during network voltage disturbances.

© 2025 by the author(s). Distributed under a Creative Commons CC BY license.

Preprints.org (www.preprints.org) | NOT PEER-REVIEWED | Posted: 4 August 2025 doi:10.20944/preprints202508.0088.v1

The discovery of the NdFeB alloy, due to its high magnetic energy, places permanent magnet synchronous motors at the top of the hierarchy in terms of energy parameters and torque/mass ratio, but the currently quite high price of these magnets makes their use limited in the medium and low power range.

Below are some examples of permanent magnet synchronous motor (PMSM) constructions with radial air gap.

The stator of these motors is structurally identical to that of induction motors, being made of electrical steel sheets, with notches in which the stator winding is distributed. **Figure 1** shows the general construction of a radial air gap MSPM.

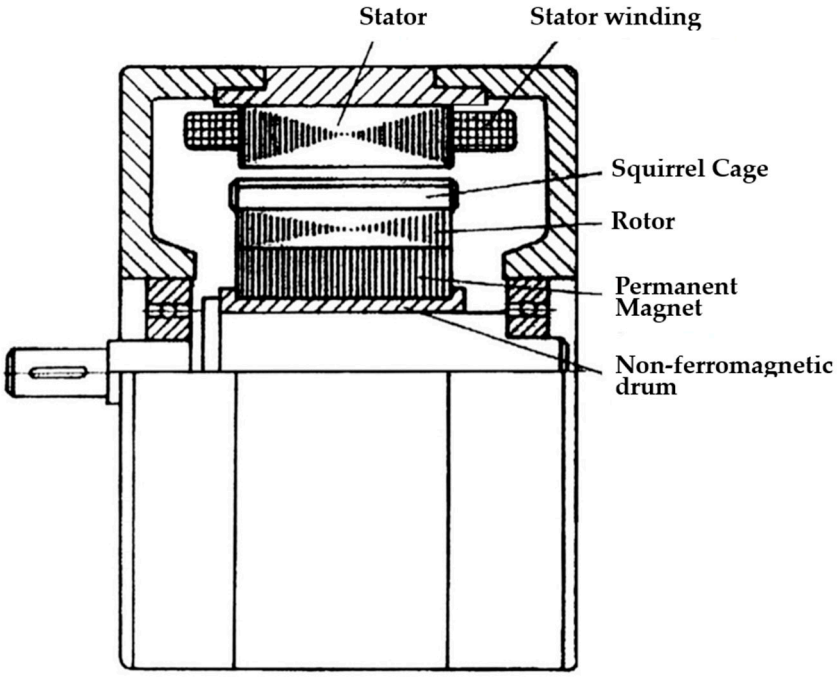

Figure 1. Permanent magnet synchronous motor with radial electromagnetic field.

There is a wide variety of constructive solutions for the cylindrical rotor, some of which are presented below.

The cylindrical rotor of these machines can be made in normal construction (**Figure 2**a) or with salient poles and squirrel cage into a common construction (**Figure 2**b).

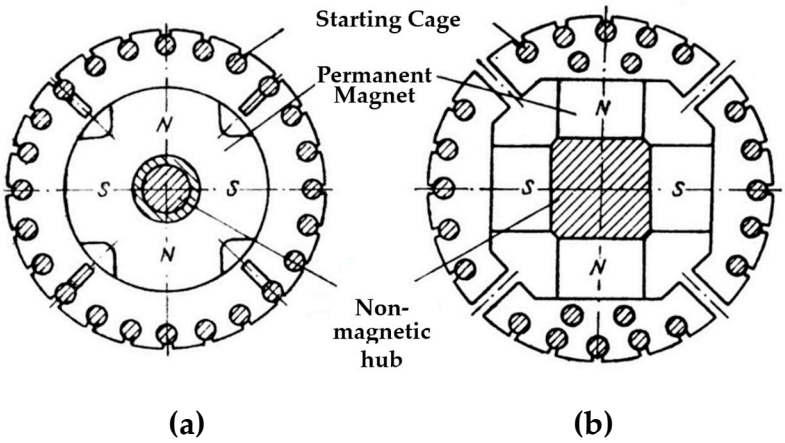

Figure 2. Various rotor designs of permanent magnet motors. **(a)** Normal design; **(b)** With salient poles and squirrel cage.

© 2025 by the author(s). Distributed under a Creative Commons CC BY license.

Preprints.org (www.preprints.org) | NOT PEER-REVIEWED | Posted: 4 August 2025 doi:10.20944/preprints202508.0088.v1

Figure 3a shows a constructive solution that uses permanent magnets, placed radially and circularly to increase the magnet surface area per pole and achieve the greatest possible concentration of the induction field.

The constructive solution presented in **Figure 3**b, with the magnets arranged in a zig-zag pattern, achieves the highest concentration ratio (the ratio between the active magnet surface area and the surface area of a pole) for a four-pole construction, but has the disadvantage of a relatively high rotor leakage coefficient.

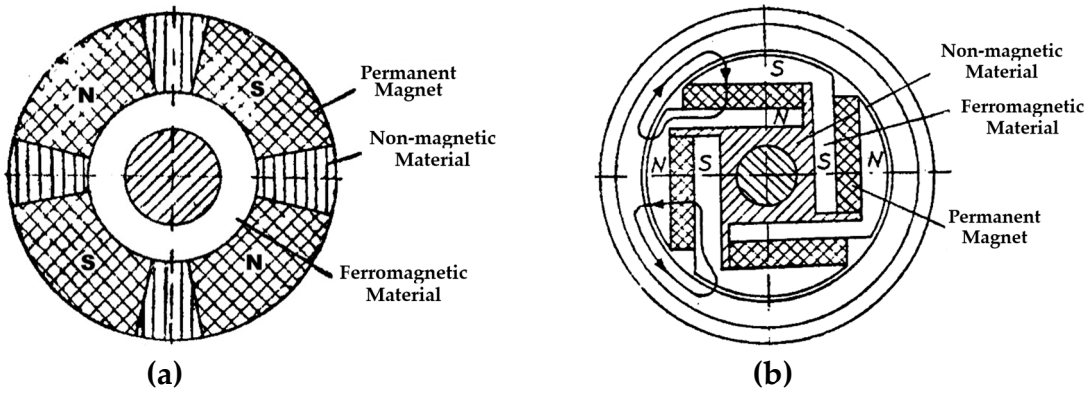

Figure 3. Permanent magnet rotor. **(a)** Circular arrangement; **(b)** Zig-zag arrangement.

Figure 4a and **Figure 4**b show two rotor designs derived from variable reluctance motor rotors with flux barriers, where permanent magnets were introduced instead of the barriers.

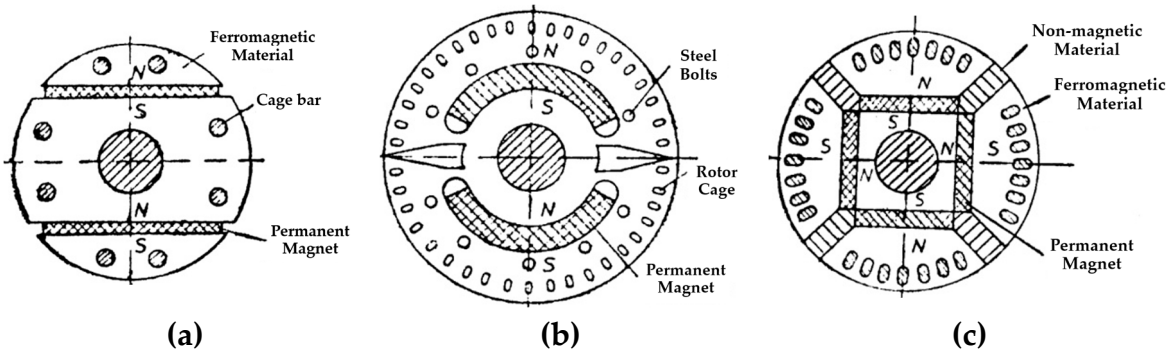

Figure 4. Rotor with permanent magnets. **(a)** Positioned on the chord; **(b)** In the form of circular segments; **(c)** In polygonal form, with field weakening.

It is observed that the pole area is larger than the magnet area and the magnet height is smaller, which suggests that the solution is only suitable for the use of rare earth magnets, which, having relatively high remanent inductions and coercive field intensities, are suitable for relatively small magnet areas and heights, as can be seen from the figure.

Another constructive solution that uses high-energy permanent magnets, based on samarium or neodymium, is the one in **Figure 4**c, for a four-pole motor.

The constructive solutions shown in **Figures 4**a, **4**b and **4**c also have a cage placed radially over the permanent magnets. This cage has a starting role, if the motor is used as a synchronous motor with permanent magnets powered by the 50 Hz network, operating at constant speed [16–19].

In the case of motors intended to operate in variable speed drive systems, systems that also control the internal angle, the presence of the cage for starting is no longer necessary. If permanent magnets with a high coercive magnetic field intensity value are used in these motors, such as those based on samarium or neodymium, then the presence of the cage is no longer necessary for its shielding role and can be dispensed with.

© 2025 by the author(s). Distributed under a Creative Commons CC BY license.

Preprints.org (www.preprints.org) | NOT PEER-REVIEWED | Posted: 4 August 2025 doi:10.20944/preprints202508.0088.v1

AC motors with double stators or rotors and permanent magnets are known in the literature, but their construction is quite complicated and they are generally made for use in the field of electric vehicles. [20–22].

In the paper [23] presented by Aymen Flah et al. it is shown that the use of AC motors for EVs allows the creation of advanced circuit topologies to suit machines with two rotors or two stators. In the paper, two control configurations of electric machines for EVs are presented and their advantages and disadvantages are discussed, and the corresponding mathematical models were developed to improve a Field-Oriented Control (FOC) strategy.

Jiacheng Wu et al. in [24] conduct a comparative study between the single-stator permanent magnet synchronous motor (SS-PMSM) and the double-stator permanent magnet synchronous motor (DS-PMSM), which can make maximum use of the space in the motor cavity to have a higher torque density, thus being more suitable for direct drive situations with low speed and high torque.

In [25] Kwang-Il Jeong et al. present a new double-gap surface-mounted permanent magnet synchronous motor (DAG-SPMSM) and investigate its electromagnetic characteristics. The motor consists of two stators (inner and outer) and a single rotor with permanent magnets on both sides (inner and outer). The magnets are arranged in a zig-zag configuration to isolate the inner and outer magnets of the stator and rotor.

Minchen Zhu et al. consider in [26] that the double stator permanent magnet machine (DSPM) has been shown to have high space utilization and redundant structure, which can be beneficial for improving fault tolerance and torque density performance. In the paper, three configurations of double stator machines are proposed and compared, for which two sets of armature windings are wound in both stators, inner and outer, producing a higher torque component compared to single stator PM machines.

In the study presented in [27] Zhitong Ran et al. compare the electromagnetic performance of radial flux, double rotor, permanent magnet machines (DRPM) with series (S) and parallel (P) magnetic circuits for two rotors, i.e. SDRPM and PDRPM, considering different combinations of slot/pole numbers, stator winding configurations and machine dimensions. The machines are optimized using finite element analysis (FEA) based on genetic algorithms.

The object of the study presented in this paper is the validation of a new structure of an alternating current machine in the synchronous version, characterized by a double stator and a single rotor with radial air gap. The rotor has high specific energy permanent magnets of the NdFeB type glued on both surfaces.

Initially, in a previous work published in *Energies* [28], we dealt with the asynchronous variant, for which, between the two stators with series-connected windings, a rotor consisting of a cage made of copper bars or cast aluminum rotates. The active surface of a classical asynchronous machine is made up of the notches-gap-bars area, the armature yokes serving to close the flux. In the new structure, the reunion of two active areas of different diameters in a single construction was considered. This machine could be equivalent to two elementary machines coupled on the same shaft if the dimensions of the active areas and their operation were not affected by the reunion.

The flanged construction of the rotor, along with its reduced radial thickness, ensures reduced inertia. However, its mechanical construction must be very carefully studied to ensure perfect concentricity. Finally, given that the flux in the machine is dictated by the total cross-sectional area of the teeth in the inner stator, it can be stated that the asynchronous motor with two stators develops double the torque compared to a standard motor in reverse construction, consisting of the inner stator and the rotor cage.

The synchronous structure we propose in this paper is equivalent to two classical permanent magnet synchronous machines, electrically connected in series and coupled on the same shaft. These elementary machines operate at the same autopilot angle, but their power factors and internal angles differ. Overall, however, the structure with the two stators behaves like a classical permanent magnet synchronous machine.

© 2025 by the author(s). Distributed under a Creative Commons CC BY license.

Preprints.org (www.preprints.org) | NOT PEER-REVIEWED | Posted: 4 August 2025 doi:10.20944/preprints202508.0088.v1

2. Materials and Methods

Although the solution of the asynchronous motor with two stators and a massive rotor is inefficient compared to a standard motor (the efficiency does not exceed 70% due to the high resistivity of the massive rotor), it paved the way for a synchronous variant of the machine with two stators and a single rotor, using rare-earth permanent magnets, which are arranged on both cylindrical surfaces of the rotor.

In this way, the volume of the magnets and the flux of the machine can be increased.

The rotor construction, by massive steel, mechanically robust, does not pose any problems in terms of electromagnetic aspects, because it rotates synchronously with the component of the fundamental stator field, which no longer induces eddy currents in the rotor iron in a permanent manner.

The stator windings are of the classic type, with a shortened pitch, in two layers. They represent the inductor for the asynchronous version and the induced one for the synchronous version. The number of turns is imposed by the voltage applied to the terminals and by the flux determined by the total section of the inner teeth.

Regarding the connection method of the coils of the two stators, several variants were studied, finally being preferred those in **Figure 5**.

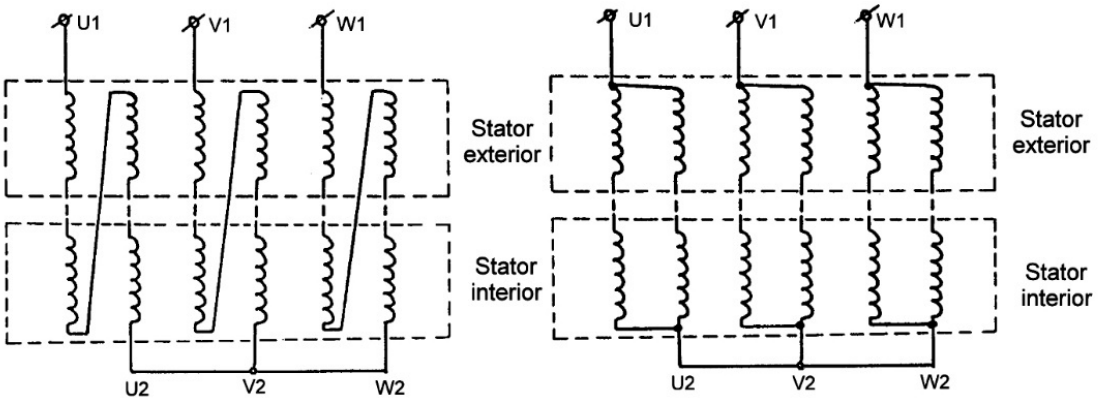

Figure 5. Connection diagram of the stator windings. **(a)** Asynchronous version; **(b)** Synchronous version.

For the asynchronous version, a series connection of the windings of the two stators and a star connection (Y) of the three phases was adopted. The coils are distributed equally on the two stators, but a distribution different from 50% is also possible (for example 40% in the inner armature and 60% in the outer one) without influencing the machine's performance decisively.

In the synchronous version, the fluxes are more important, for the same stator construction, and the e.m.f. exceeds 220 V per phase in the case of the connections in **Figure 5**a.

This is important for operation as a synchronous motor, when the supply voltages cannot exceed this value.

Therefore, for this case, the connection in **Figure 5**b was chosen, with the parallel connection of the series coil groups of the two stators on each phase. The possibility of parallel connection between the two stators is excluded due to the circulating currents that could appear due to differences between the induced e.m.f.

In **Figure 6** the lines of the inductor magnetic field, at no-load operation, are represented for the two variants, asynchronous and synchronous

© 2025 by the author(s). Distributed under a Creative Commons CC BY license.

Preprints.org (www.preprints.org) | NOT PEER-REVIEWED | Posted: 4 August 2025 doi:10.20944/preprints202508.0088.v1

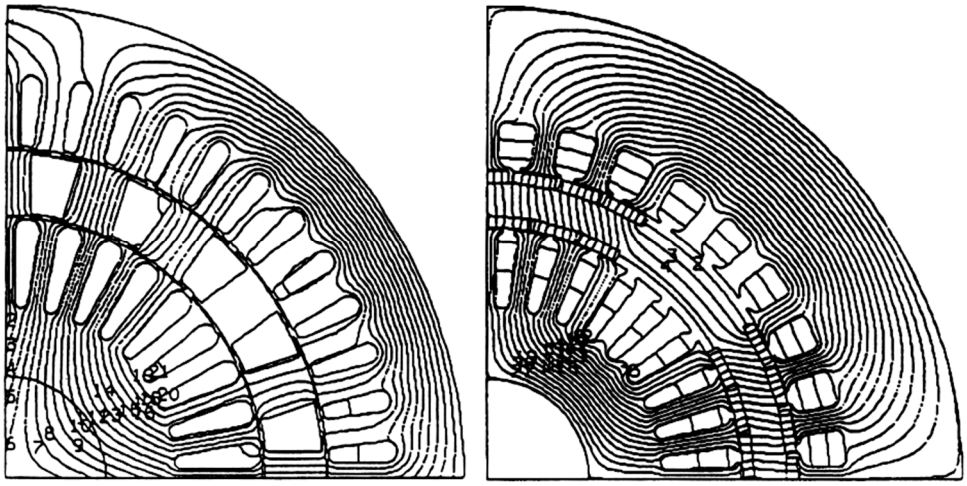

(a) **(b)**

Figure 6. Magnetic flux during no-load operation in the double-stator machine. **(a)** Asynchronous variant; **(b)** Synchronous variant.

As can be seen, in the synchronous version, part of the inductor flux is closed through the rotor, which can be advantageous for the optimal use of the machine's active surfaces.

2.1. Technological and Constructive Problems of the Tubular Rotor with Permanent Magnets

2.1.1. Choosing the Type and Number of Magnets

The choice of the type and number of magnets to be fixed on the two bores must take into account:

- Obtaining an e.m.f. as sinusoidal as possible.
- Avoiding saturation of the stator magnetic circuits, so that iron losses remain at acceptable values.

Rare earth magnets capable of providing a value of 0.8 – 0.81 T for the fundamental induction in the air gap were considered.

The radial thickness of these permanent magnets is around 3.5 mm, being made of plates measuring 20 × 15 mm.

With this structure, 6 × 3 magnets per pole are obtained for the outer surface of the rotor and 5 × 3 magnets for the inner surface, representing a pole coverage factor of approximately 2/3 for each rotor surface.

The permanent magnets are fixed to the rotor cylinder by gluing.

At each pole, the six outer magnets are coaxial with the five inner poles.

As can be seen from **Figure 7**, the outer diameters Φ 224.4 mm and the inner diameter Φ 180 mm must be respected to avoid friction of the rotor against the two stators.

If necessary, the machining of the rotor cylinder can be corrected.

Additionally, the outer magnets can also be fixed with a layer of "polyglass" (glass fibre tape) having a thickness of 0.1 mm.

The construction allows the synchronous machine to be characterized as having sunken poles (smooth rotor). The fluxes that cross the two air gaps are different, part of the field lines closing through the massive rotor.

As can be seen from **Figure 6**b, part of the flux links both stators, another part only the outer stator.

The construction details of the rotor subassembly are shown in **Figure 8**a and in the following **Figure 8**b.

© 2025 by the author(s). Distributed under a Creative Commons CC BY license.

Preprints.org (www.preprints.org) | NOT PEER-REVIEWED | Posted: 4 August 2025 doi:10.20944/preprints202508.0088.v1

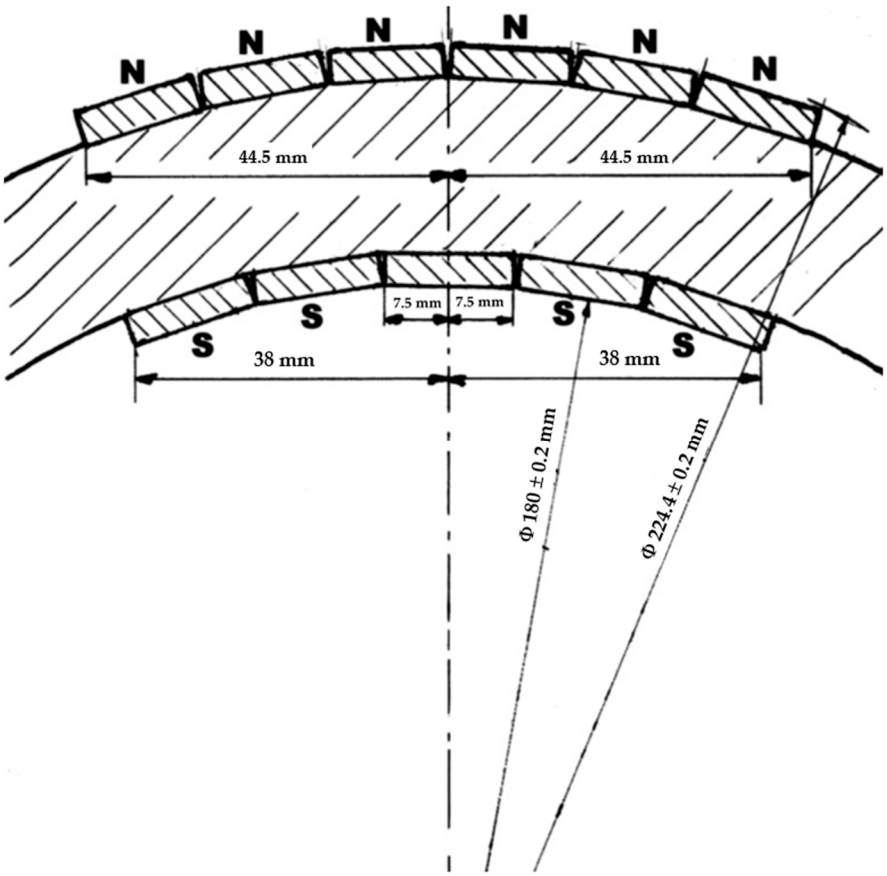

Figure 7. Permanent Magnets Attachment Method.

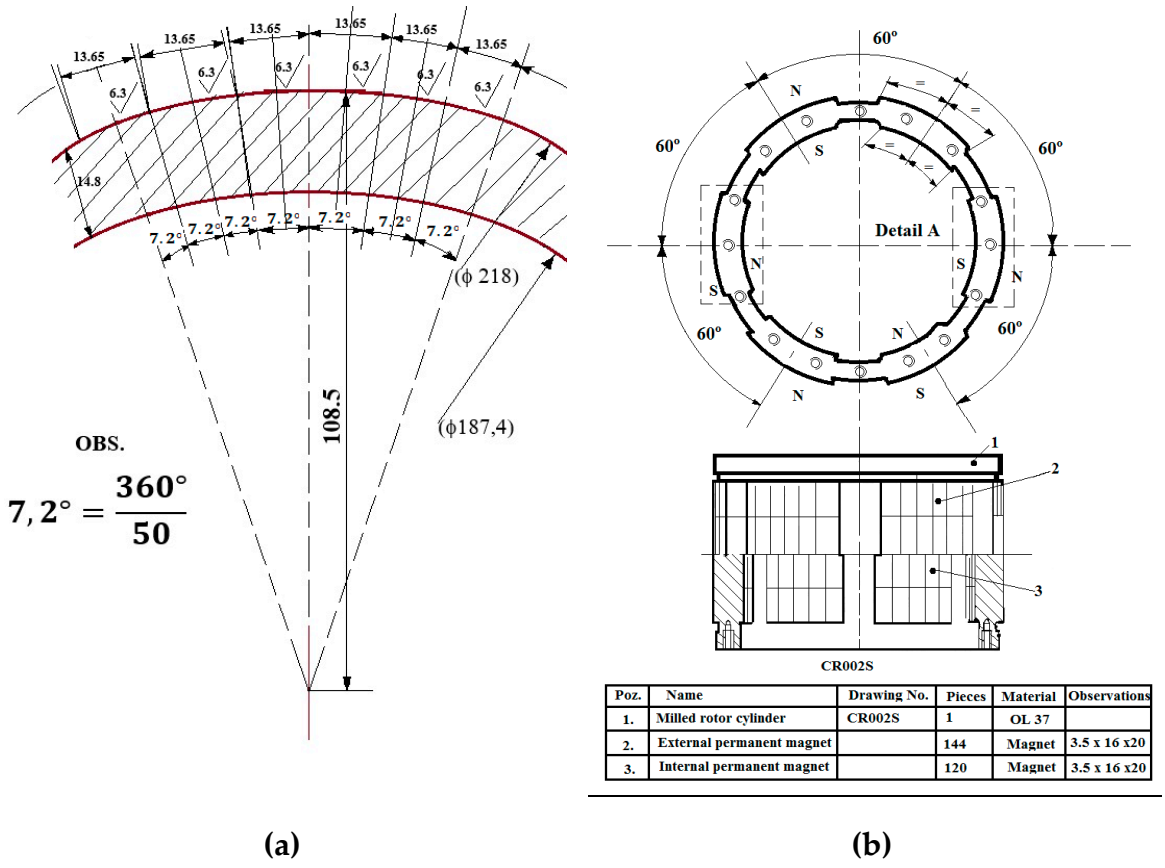

Figure 8. Construction details of the rotor subassembly. **(a)** Milled cylinder rotor; **(b)** Rotor subassembly.

© 2025 by the author(s). Distributed under a Creative Commons CC BY license.

Preprints.org (www.preprints.org) | NOT PEER-REVIEWED | Posted: 4 August 2025 doi:10.20944/preprints202508.0088.v1

The distribution of the flux depends on the opening (extension) of the permanent magnets on the inside and outside, the width of the teeth of the two stators, the radial thickness of the rotor, and, of course, the saturation of each portion of the magnetic circuit.

2.1.2. Cogging Torque

Due to the high flux and the reduced air gap, permanent magnet synchronous machines exhibit significant tooth torques, their amplitude reaching in some cases up to 30% of the nominal torque.

The periodicity of these torques, which are exerted between the rotor poles and the teeth, is of one tooth pitch, and their shape is asymmetrical in relation to the tooth axis.

Several methods are indicated in the specialized literature for reducing these torques [29–32], the best known being the inclination of the stator notches with a tooth pitch.

In a two-dimensional calculation (using a calculation program based on the finite element method), the inclination of the notches cannot be taken into account directly, and things become complicated.

The rotor should be rotated discretely, the tooth torques determined at each point, and an average over a tooth pitch calculated using the virtual things method.

During the simulations (with Flux 2D and Flux 3D software, developed by CEDRAT, which are FEM commercial software simulating electromagnetics and thermal physical phenomena), it was found that the determinations are sensitive to the discretization network used during rotor rotation, as well as the connection of nodes at the air gap level.

Thus, for certain networks, the tooth torque was no longer asymmetric.

To solve this problem, for each pair of points placed symmetrically with respect to the tooth axis, the networks were rebuilt until equal and opposite tooth torque values were obtained (differences below 3%).

In the case of the structure studied in this paper, the results are presented in **Figure 9**, separately for the inner and outer poles in **Figure 9**a and the resulting tooth torque in **Figure 9**b.

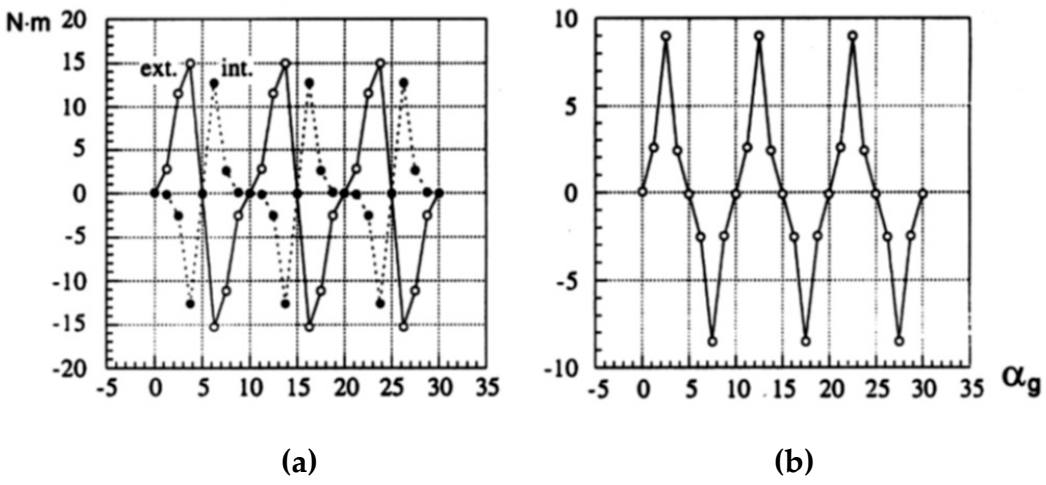

Figure 9. Cogging torque. **(a)** For inner and outer poles; **(b)** Resultant torque.

In a synchronous machine with permanent magnets arranged on the rotor surface, the cogging torque at no-load operation results solely from forces exerted at the pole edges. One tooth is positioned in the middle of the pole and, due to the symmetry of the magnetic field lines at no-load, exerts no tangential force on the rotor. Therefore, the tooth torque depends on the distance between the pole edges, that is, the magnet extension, as well as on the ratio between the width of the tooth and the notch, and on the shape of the induction in the air gap.

A significant reduction in the cogging torque is achieved by setting the opening of the permanent magnet slightly more than an integer multiple of tooth pitches. One solution is to use a rotor consisting of

© 2025 by the author(s). Distributed under a Creative Commons CC BY license.

Preprints.org (www.preprints.org) | NOT PEER-REVIEWED | Posted: 4 August 2025 doi:10.20944/preprints202508.0088.v1

N sectors (in the longitudinal direction) offset from each other by td/N, where td is the tooth pitch. This way, all the harmonics of the tooth torque are cancelled, except for the harmonics that are multiples of N.

Another solution proposes a progressive air gap to make the induction in the air gap as sinusoidal as possible. The sudden, stepwise variation of the induction is completely unfavorable. About the above, the inclination of the notches with a stator tooth pitch, in the opposite direction for the two stators, was provided, a solution easier to achieve for a series production. This solution allows at the same time to improve the e.m.f. curve by reducing the tooth harmonics.

The considerations presented allow the establishment of a transversal geometry presented in **Figure 10**, for the two variants: asynchronous **(a)** and synchronous **(b)**.

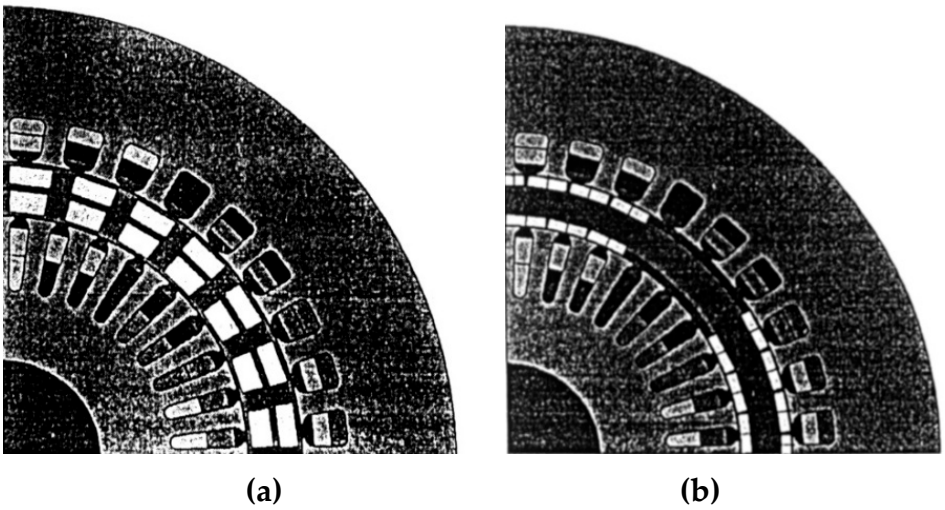

Figure 10. Proposed transverse geometry. **(a)** Asynchronous variant; **(b)** Synchronous variant.

The idea of the new structure consists in combining two machines with different air gap diameters, each consisting of classical active zones (notches – air gap – bars, for the asynchronous version and notches – air gap – permanent magnets, for the synchronous one) into a single machine, keeping the two active zones and a single pair of yokes for closing the flux.

To the extent that neither the dimensions of the active zones nor the operation of each classical machine are affected by this combination, it can be said, theoretically, that the proposed machine is equivalent to the two simple machines coupled on the same shaft. In practice, however, certain complications arise.

2.2. Numerical Characterization of the Permanent Magnet Synchronous Version of the Double Stator Machine

2.2.1. Generalities

In the synchronous version, the inductor is represented by the rotor with permanent magnets fixed on both sides of a solid steel cylinder, and the induced current is produced by the two stators with connected windings. By grouping the series coils of the two stators in parallel, the e.m.f. of the machine is halved and the current is doubled, which suits the usual voltages of inverters.

It was considered an interchangeability of the two rotors, for asynchronous and synchronous versions, to facilitate experimentation and to make possible a series of comparisons of the results obtained.

The transition from an asynchronous to a synchronous version can be done by replacing the squirrel cage rotor with a permanent magnet rotor and modifying the stator winding connections.

The machine's characterization was carried out by constructing its vector diagram and calculating its parameters. This calculation can be done by simulations using the finite element method or by analytical methods.

© 2025 by the author(s). Distributed under a Creative Commons CC BY license.

Preprints.org (www.preprints.org) | NOT PEER-REVIEWED | Posted: 4 August 2025 doi:10.20944/preprints202508.0088.v1

2.2.2. Vector Diagram and Operation Under Load

The permanent magnets are fixed on the cylindrical surfaces of the rotor, and their relative permeability being close to unity (μr = 1.05), the machine can be considered with sunken poles (with a smooth rotor). In the hypothesis of a linear magnetic circuit, the equation of voltages per phase is written:

$$\underline{U} = (R_i + R_e) \cdot \underline{I} + j(X_{\sigma i} + X_{\sigma e}) \cdot \underline{I} + \underline{E}_{ri} + \underline{E}_{re} = \\ = (R_i + R_e) \cdot \underline{I} + j(X_{si} + X_{se}) \cdot \underline{I} + \underline{E}_{0i} + \underline{E}_{0e} \quad (1)$$

where R denotes the stator winding resistances, Xσ the leakage reactance, Er the resultant e.m.f. per phase, Xs the synchronous reactance and E_0 the no-load e.m.f., the indices "i" and "e" signifying internal and external stators, respectively.

The phase phasor diagram, neglecting the ohmic voltage drops ($R << X_s$), is represented in **Figure 11**. The no-load operating electromotive voltages of the two stators, E_{0i} and, respectively, E_{0e}, are clearly in phase. Both equation (1) and the phasor diagram viewed from the terminals allow us to see that the machine is equivalent to a classical permanent magnet machine.

It can be considered that the double stator machine is the result of the series connection to the network of two classical machines, which are coupled on the same shaft. If the magnetic circuit of the rotor is not saturated, the two classical machines can be physically separated by a cylindrical cut at the median level of the rotor and studied each one separately.

Through this separation, we will allow the superposition of 4 fluxes existing simultaneously in the machine, 2 inductors produced by the external and internal magnets, respectively, and 2 intrinsic fluxes of each stator winding.

The two elementary machines in which we have sectioned the machine with double stator and magnets fixed on both rotor surfaces operate with the same autopilot angle Ψ, but their power factors and internal angles will be different, because the ratio between the electro motive forces at no-load operation and the synchronous reactances of the two machines is not the same.

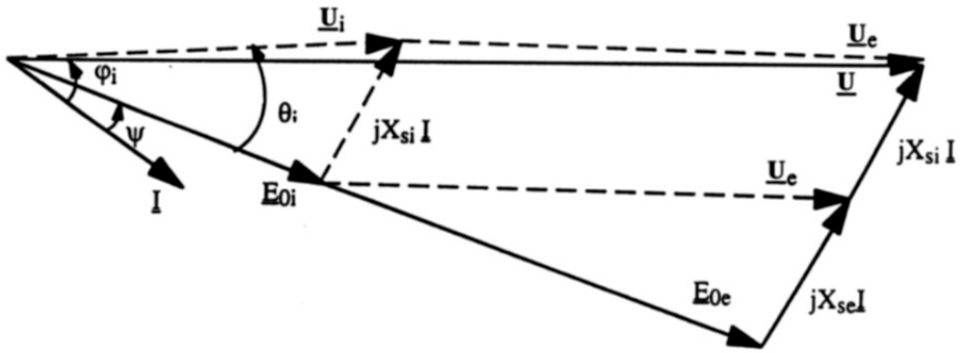

Figure 11. Phasor diagram for load operating.

2.2.3. Synchronous Reactance of the Machine

The three-phase stator windings, fed with a balanced system of currents, produce a rotating field that induces e.m.f. in their own phases. The voltages are proportional to the currents I that flow through each phase and can be interpreted as an inductive voltage drop X_{aI} at the terminals of a reactance, which is the useful cyclic reactance on phase Xa. The synchronous reactance is the sum of Xa and the leakage reactance on phase Xσ (due mainly to the coil ends).

Figure 12 shows the distribution of the induced reaction flux, in the d-axis, in the absence of the inductor flux.

© 2025 by the author(s). Distributed under a Creative Commons CC BY license.

Preprints.org (www.preprints.org) | NOT PEER-REVIEWED | Posted: 4 August 2025 doi:10.20944/preprints202508.0088.v1

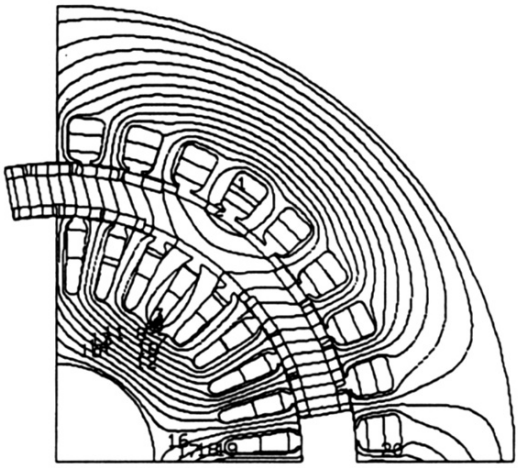

Figure 12. Distribution of the induced reaction flux in the d-axis, in the absence of the inductive flux.

Because of the very high reluctance of the magnets, the induced reactance is lower than in the electromagnetically excited synchronous machine, in which the air gap reluctance constitutes the predominant term in the total reactance of the circuit.

Therefore, the synchronous reactance of permanent magnet machines is lower and the assumption of neglecting resistances in addition to the synchronous reactances must be made with some caution. In fact, the phase resistance of the stator winding can reach 10% of the synchronous reactance.

2.3. Analytical Model

Analytical models do not require the calculation of the field distribution in the studied structures and allow a flexible, rapid, and sufficiently precise analysis of the influence of various geometric or material parameters on the machine characteristics. Obviously, they suffer from a lack of information about what is happening at local levels.

An analytical model adapted to the proposed construction, with magnets fixed on the rotor surface, reduces the calculation to the active area of the machine, consisting of magnets, air gap and the tooth-notch regions. The yokes are considered to have infinite permeability, but the finite permeability of the stator teeth is taken into account. The permanent magnets are represented by a surface charge density, placed in front of the magnet, according to the Coulombian model. The principle of the model consists in the analytical calculation of the field created by the stator.

The electromagnetic torque results from the interaction between this field and the representative magnetic charges of the permanent magnets. The calculation of the stator field is performed in a simplified geometry, obtained by homogenizing the magnet-air gap region on the one hand and the tooth-notch region on the other hand.

The discrete distribution of the current density in the notches is taken into account. The permeability homogenization of the magnet-gap zone and the tooth-notch zone is performed for an elementary cell equal to one tooth pitch, comprising a stator notch framed by two tooth halves and placed under the rotor magnet.

After homogenization, the rotor becomes smooth.

The calculations are performed under the following simplifying assumptions (in addition to the above):

• Firstly, it is a two-dimensional analysis in which we consider the area of interest to be straight; therefore, the curvature of the bore, as well as end effects, are neglected.

• Secondly, we consider permanent magnets rigid and magnetized in a single direction; their magnetization does not vary in space and remains equal to the remanent one, whatever the demagnetizing fields, if it remains below its critical value Hcr. Each magnet is replaced by superficial

© 2025 by the author(s). Distributed under a Creative Commons CC BY license.

Preprints.org (www.preprints.org) | NOT PEER-REVIEWED | Posted: 4 August 2025 doi:10.20944/preprints202508.0088.v1

magnetic masses, whose density σ at each point on the magnet surface is defined by being the external normal to the magnet surface.

• Thirdly, the field in the air gap has the same amplitude in no-load and load conditions; the stator tooth material then has a fixed permeability, determined by the chosen operating point.

2.4. Thermal Considerations

The existence of the two air gaps as heat barriers by interposing the inner stator instead of the rotor yoke of standard asynchronous motors creates the possibility of producing significant local heating. That is why it seemed necessary to develop an appropriate thermal model for the new proposed structure.

An analogy with an electrical diagram with concentrated parameters was used: the current sources correspond to the power dissipated in various parts in contact; then the electrical voltages correspond to the temperature differences, respectively the heating.

The calculations confirmed the fear that, under conditions of similar current densities, the heating of the inner stator winding exceeds that of the outer winding by about 20°C, which imposed some measures related to the ventilation of the machine.

2.5. Simulation Results for the Two-Stator and One-Tubular-Rotor Permanent Magnet Synchronous Motor

The simulation results of the three-phase permanent magnet synchronous motor with two stators and a single rotor are presented below. The cross-sectional geometry and the discretization mesh, with approximately 46,000 nodes, are also presented.

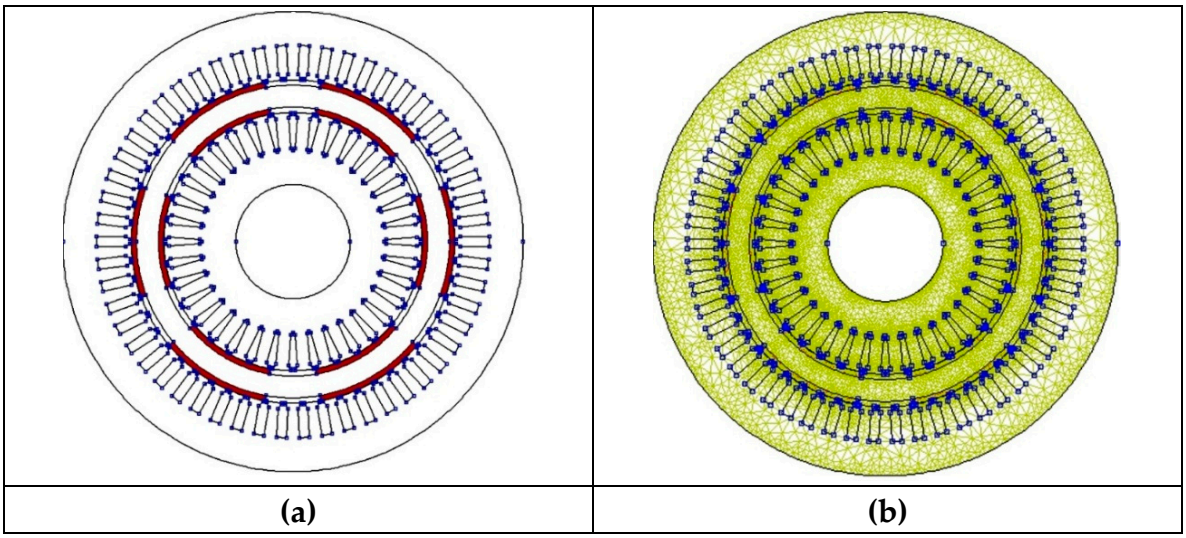

Figure 13. Three-phase synchronous motor with two stators and a single rotor, with permanent magnets. **(a)** Transverse geometry; **(b)** Discretization network.

© 2025 by the author(s). Distributed under a Creative Commons CC BY license.

Preprints.org (www.preprints.org) | NOT PEER-REVIEWED | Posted: 4 August 2025 doi:10.20944/preprints202508.0088.v1

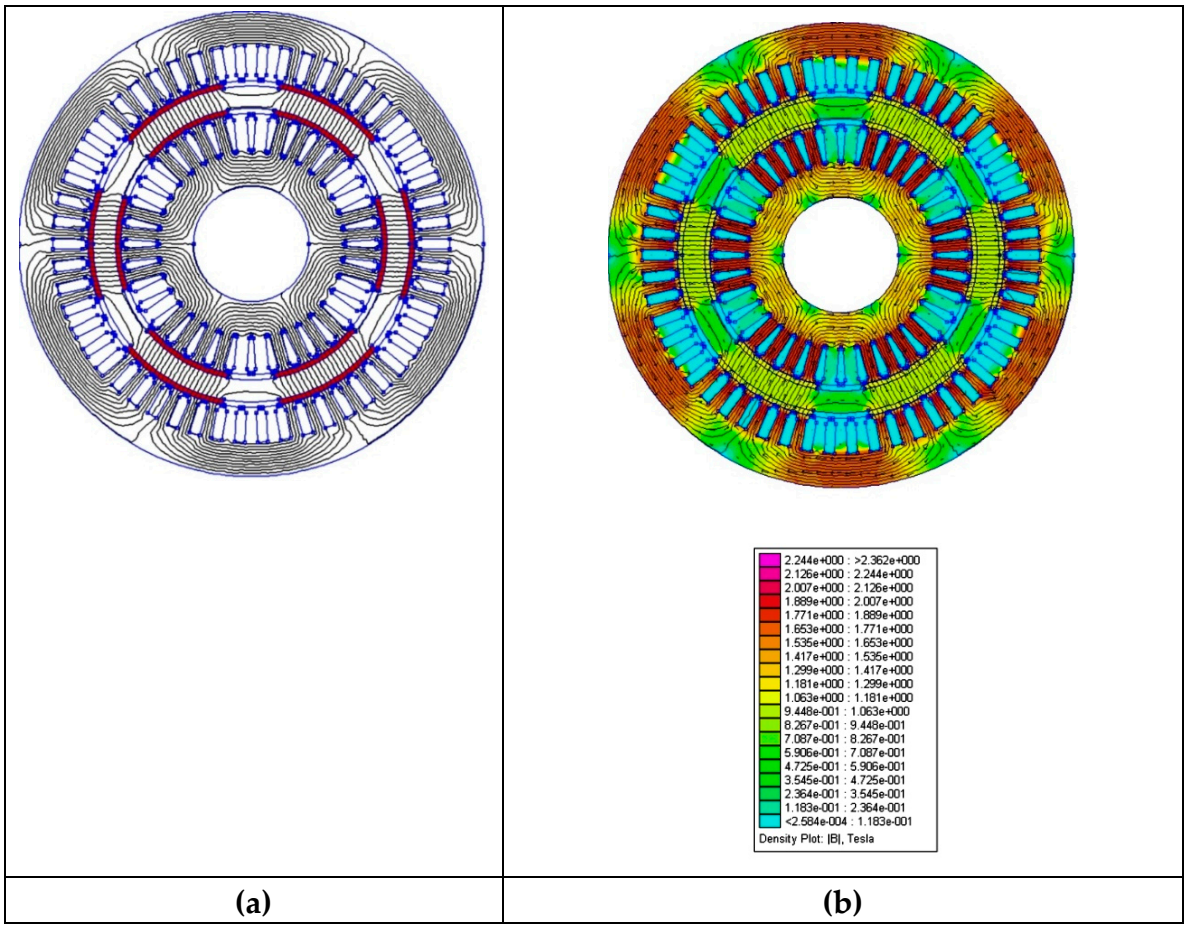

Figure 14. Three-phase synchronous motor with two stators and a single rotor, with permanent magnets. **(a)** Magnetic flux paths at no-load operation; **(b)** Magnetic induction values at no-load operation.

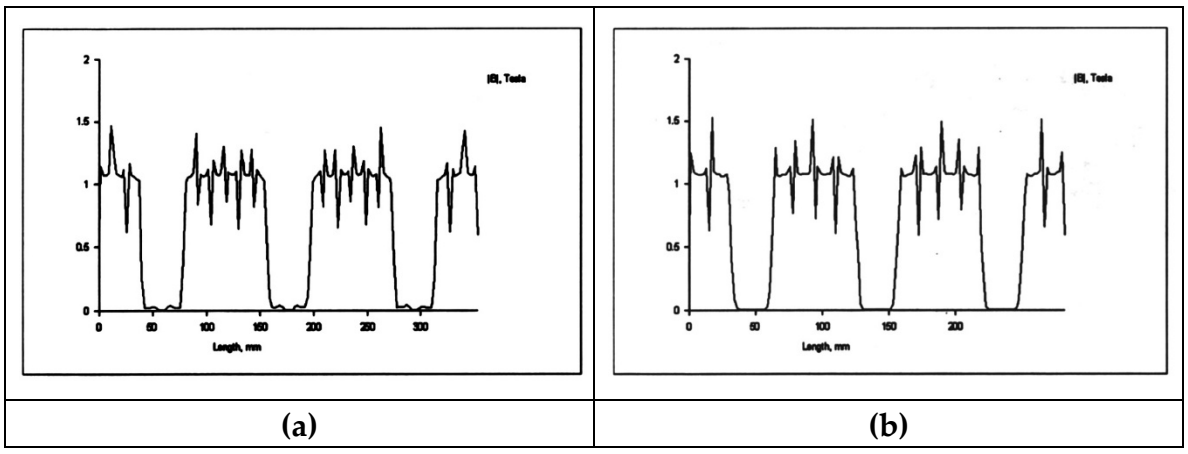

Figure 15. Three-phase synchronous motor with two stators and a single rotor, with permanent magnets. **(a)** Magnetic induction in the outer air gap; **(b)** Magnetic induction in the inner air gap.

Thus, previously, we present some of the simulation results for the two-stator tubular-rotor permanent magnet synchronous motor using QuickField™ 6.0 software, which is an efficient finite element analysis package for electromagnetic, thermal, and stress design simulation with a multi-analysis coupled field.

© 2025 by the author(s). Distributed under a Creative Commons CC BY license.

Preprints.org (www.preprints.org) | NOT PEER-REVIEWED | Posted: 4 August 2025 doi:10.20944/preprints202508.0088.v1

3. Execution and Certification of the Experimental Prototype

3.1. Certification of the Prototype of a Permanent Magnet Synchronous Motor with a Tubular Rotor

After preliminary calculations, and computer simulations, an execution project for the prototype of an asynchronous motor with double stator and tubular rotor in cage were carried out and then the prototype of the motor with double stator and tubular rotor in asynchronous version, with double cage with round bars, was built in collaboration with the prototype workshop at S.C. UMEB S.A., following what was shown in this paper, it emerged that a synchronous version with permanent magnets would be even more efficient than the asynchronous one under the conditions in which, in any case, the stator subassembly remains unchanged.

Consequently, an interchangeable rotor was executed composed of a massive steel tube on which were glued, on both the outer and inner bore, plates of high magnetic energy permanent magnets, produced at S.C. ICPE S.A. (laboratory of Dr. W. Kappel).

3.2. Carrying Out Tests in the Laboratory of Prototypes from S.C. UMEB S.A. and Test Reports with Experimental Results

As for the asynchronous version, the laboratory tests and trials for the synchronous version were also carried out in the prototype laboratory of S.C. UMEB S.A. The test program and the results obtained are presented below:

SAMPLES PROGRAM

1. Coupling the synchronous machine with a DC motor.

2. Testing the synchronous machine as a generator with no-load operation.

3. Gradually rotating at a speed of 1000 rpm, the voltages at the terminals of the synchronous machine operating in no-load mode will be measured for different types of connections and between various points.

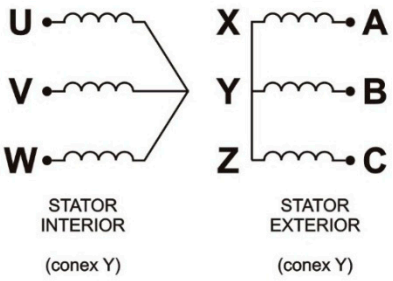

(a)

U_{AB}
U_{BC}
U_{CA}
U_{AX}
U_{BY}
U_{CZ}
U_{UV}
U_{VW}
U_{WB}

Connecting terminals A and U and measuring voltages:

U_{AV} U_{AW} U_{CV}

U_{BW} U_{BV} U_{CW}

(b)

Connecting terminals A and V and measuring voltages:

U_{BV} U_{BW} U_{AV}

U_{CU} U_{CW} U_{AW}

(c)

Connecting terminals A and W and measuring voltages:

U_{AU} U_{AV}

U_{CU} U_{CW}

U_{CU} U_{CV}

(d)

Connecting terminals B and V and measuring voltages:

U_{AU} U_{AW}

U_{CW} U_{CU}

(e)

© 2025 by the author(s). Distributed under a Creative Commons CC BY license.

Preprints.org (www.preprints.org) | NOT PEER-REVIEWED | Posted: 4 August 2025 doi:10.20944/preprints202508.0088.v1

Connecting terminals B and W and measuring voltages:

U_{AU} U_{AV}

U_{CU} U_{CV}

(f)

Connecting terminals C and U and measuring voltages:

U_{AV} U_{AW}

U_{BV} U_{BW}

(g)

Figure 16. Measurement of voltages at the terminals of the synchronous machine operating in no-load mode for different types of connections. **(a)** Schematic diagram; **(b)** Connection of terminals A and U; **(c)** Connection of terminals A and V; **(d)** Connection of terminals A and W; **(e)** Connection of terminals B and V; **(f)** Connection of terminals B and W; **(g)** Connection of terminals C and U.

4. Testing the synchronous machine as a generator in no-load operation.

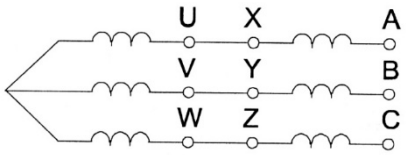

U_{AB}

U_{BC}

U_{CA}

5. Spinning at 1000 RPM and with the connection:

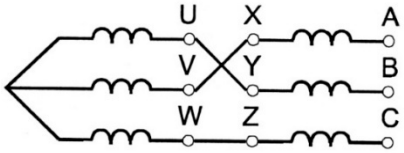

U_{AB}

U_{BC}

U_{CA}

6. Spinning at 1000 RPM and with the connection:

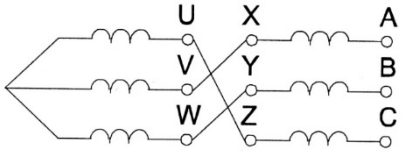

U_{AB}

U_{BC}

U_{CA}

DOUBLE STATOR PERMANENT MAGNET SYNCHRONOUS MOTOR MEASUREMENT

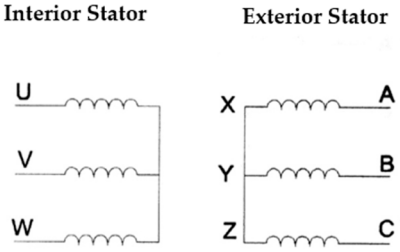

Right-hand axis

N = 100 r/min

(33,33 Hz)

Y – Y Connection

U_{AB}	88,5 × 8	708 V
U_{BC}	88,5 × 8	708 V
U_{CA}	88,5 × 8	708 V
U_{AX}	82 × 5	410 V
U_{BY}	82 × 5	410 V
U_{CZ}	82 × 5	410 V
U_{UV}	125 × 2	250 V
U_{YW}	125 × 2	250 V
U_{UW}	125 × 2	250 V

(a)

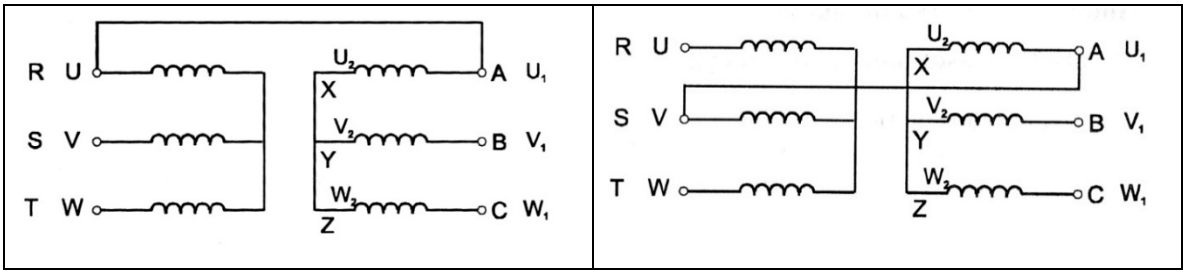

© 2025 by the author(s). Distributed under a Creative Commons CC BY license.

Preprints.org (www.preprints.org) | NOT PEER-REVIEWED | Posted: 4 August 2025 doi:10.20944/preprints202508.0088.v1

$U_{CV} \rightarrow 102 \times 8 = 816$ V $U_{BW} \rightarrow 102 \times 8 = 816$ V $U_{BV} \rightarrow 71 \times 8 = 568$ V $U_{CW} \rightarrow 119 \times 8 = 952$ V	$U_{BU} \rightarrow 112 \times 8 = 896$ V $U_{BW} \rightarrow 118,5 \times 8 = 948$ V $U_{CU} \rightarrow 84,8 \times 8 = 678,4$ V $U_{CW} \rightarrow 112 \times 8 = 896$ V
(b)	**(c)**

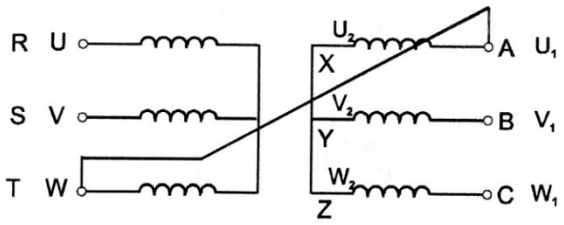 $U_{BV} \rightarrow 932,5 \times 5 = 466$ V $U_{BU} \rightarrow 136 \times 5 = 680$ V $U_{CU} \rightarrow 93,5 \times 5 = 465$ V $U_{CV} \rightarrow 135,5 \times 5 = 677,5$ V	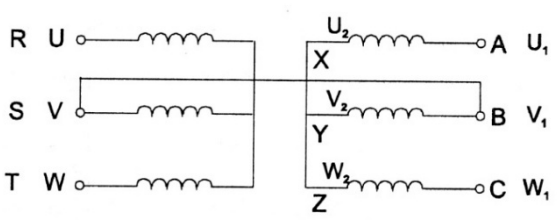 $U_{AU} \rightarrow 113,5 \times 5 = 565$ V $U_{AW} \rightarrow 93,2 \times 5 = 466$ V $U_{CU} \rightarrow 93,5 \times 5 = 465$ V $U_{CW} \rightarrow 135,5 \times 5 = 676,5$ V
(d)	**(e)**

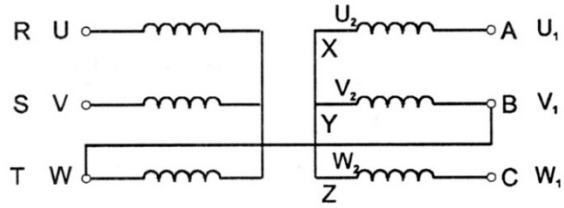 $U_{AU} \rightarrow 112 \times 8 = 896$ V $U_{AV} \rightarrow 118,5 \times 8 = 948$ V $U_{CU} \rightarrow 113,5 \times 5 = 567,5$ V $U_{CV} \rightarrow 102 \times 8 = 816$ V	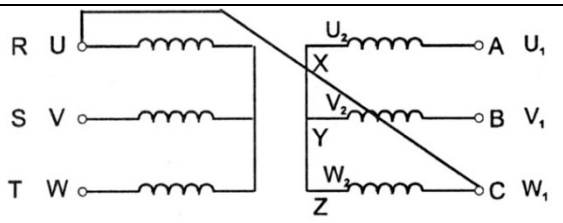 $U_{AV} \rightarrow 135 \times 5 = 675$ V $U_{AW} \rightarrow 93,5 \times 5 = 467,5$ V $U_{BV} \rightarrow 93,5 \times 5 = 467,5$ V
(f)	**(g)**

© 2025 by the author(s). Distributed under a Creative Commons CC BY license.

Preprints.org (www.preprints.org) | NOT PEER-REVIEWED | Posted: 4 August 2025 doi:10.20944/preprints202508.0088.v1

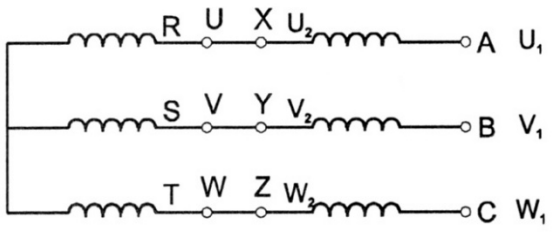

$U_{AB} \rightarrow 111,5 \times 8 = 892$ V

$U_{BC} \rightarrow 101,5 \times 8 = 812$ V

$U_{CA} \rightarrow 93 \times 5 = 465$ V

(h)

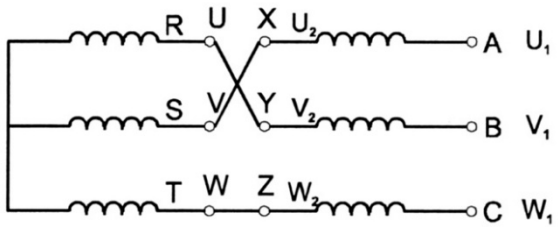

$U_{AB} \rightarrow 113 \times 5 = 565$ V

$U_{BC} \rightarrow 113 \times 5 = 565$ V

$U_{CA} \rightarrow 113 \times 5 = 565$ V

(i)

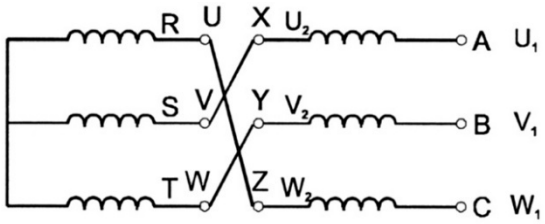

$U_{AB} \rightarrow 93,5 \times 5 = 467,5$ V

$U_{BC} \rightarrow 112 \times 8 = 896$ V

$U_{CA} \rightarrow 101,5 \times 8 = 812$ V

(j)

Figure 17. Schemes for measuring voltages at no-load in generator mode. **(a)** ÷ **(j)** Different types of connections and their corresponding voltages.

Below, the complete results of the measurements contained in the test reports prepared by the Laboratory of the Research Center of SC UMEB SA are presented.

© 2025 by the author(s). Distributed under a Creative Commons CC BY license.

Preprints.org (www.preprints.org) | NOT PEER-REVIEWED | Posted: 4 August 2025 doi:10.20944/preprints202508.0088.v1

THREE-PHASE PERMANENT MAGNETS SYNCHRONOUS MACHINE WITH DOUBLE STATOR

TEST BULLETIN NO. 1

MEASUREMENT OF OHMIC RESISTANCE

The determination was carried out at an ambient temperature of 19 °C. The meaning of the marking of the terminals between which the measurements were made is specified in the diagram below.

Outer stator Inner stator

MEASUREMENT RESULTS

The terminals between which the measurements were made	Resistance value [Ω]
U1-U2	1.4235
V1-V2	1.4211
W1-W2	1.4245
R-S	1.0542
S-T	1.0591
T-R	1.0502

THREE-PHASE PERMANENT MAGNETS SYNCHRONOUS MACHINE WITH DOUBLE STATOR

TEST BULLETIN NO. 2

NO-LOAD TEST AS A GENERATOR

Winding connection

Speed n = 1000RPM
Frequency f=50Hz

Voltage values at the various terminals

Voltage between terminals	Unit of measurement	Value
U1-U2	[V]	410
V1-V2	[V]	410
W1-W2	[V]	410
V1-W1	[V]	708
W1-U1	[V]	708
W1-W2	[V]	708
R-S	[V]	250
S-T	[V]	250
T-R	[V]	250
U1-R	[V]	
U1-S	[V]	
U1-T	[V]	
V1-R	[V]	
V1-S	[V]	
V1-T	[V]	
W1-R	[V]	
W1-S	[V]	
W1-T	[V]	
U2-V2	[V]	0
V2-W2	[V]	0
W2-U2	[V]	0

THREE-PHASE PERMANENT MAGNETS SYNCHRONOUS MACHINE WITH DOUBLE STATOR

TEST BULLETIN NO. 3

*NO-LOAD TEST AS A GENERATOR

Winding connection

Speed n = 1000RPM
Frequency f=50Hz

Voltage values at the various terminals

Voltage between terminals	Unit of measurement	Value
U1-U2	[V]	410
V1-V2	[V]	410
W1-W2	[V]	410
U1-V1	[V]	708
V1-W1	[V]	708
W1-U1	[V]	708
R-S	[V]	250
S-T	[V]	250
T-R	[V]	250
U1-R	[V]	0
U1-S	[V]	250
U1-T	[V]	250
V1-R	[V]	708
V1-S	[V]	568
V1-T	[V]	816
W1-R	[V]	708
W1-S	[V]	816
W1-T	[V]	452
U2-V2	[V]	0
V2-W2	[V]	0
W2-U2	[V]	0

THREE-PHASE PERMANENT MAGNETS SYNCHRONOUS MACHINE WITH DOUBLE STATOR

TEST BULLETIN NO. 4

NO-LOAD TEST AS A GENERATOR

Winding connection

Speed n = 1000RPM
Frequency f=50Hz

Voltage values at the various terminals

Voltage between terminals	Unit of measurement	Value
U1-U2	[V]	410
V1-V2	[V]	410
W1-W2	[V]	410
U1-V1	[V]	708
V1-W1	[V]	708
W1-U1	[V]	708
R-S	[V]	250
S-T	[V]	250
T-R	[V]	250
U1-R	[V]	250
U1-S	[V]	0
U1-T	[V]	250
V1-R	[V]	896
V1-S	[V]	708
V1-T	[V]	948
W1-R	[V]	679
W1-S	[V]	708
W1-T	[V]	896
U2-V2	[V]	0
V2-W2	[V]	0
W2-U2	[V]	0

© 2025 by the author(s). Distributed under a Creative Commons CC BY license.

Preprints.org (www.preprints.org) | NOT PEER-REVIEWED | Posted: 4 August 2025 doi:10.20944/preprints202508.0088.v1

THREE-PHASE PERMANENT MAGNETS SYNCHRONOUS MACHINE WITH DOUBLE STATOR

TEST BULLETIN NO. 5

NO-LOAD TEST AS A GENERATOR

Winding connection

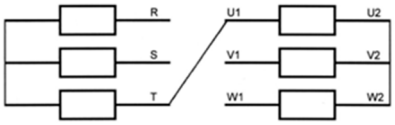

Speed n = 1000RPM
Frequency f=50Hz

Voltage values at the various terminals

Voltage between terminals	Unit of measurement	Value
U1-U2	[V]	410
V1-V2	[V]	410
W1-W2	[V]	410
U1-V1	[V]	708
V1-W1	[V]	708
W1-U1	[V]	708
R-S	[V]	250
S-T	[V]	250
T-R	[V]	250
U1-R	[V]	250
U1-S	[V]	250
U1-T	[V]	0
V1-R	[V]	680
V1-S	[V]	466
V1-T	[V]	708
W1-R	[V]	465
W1-S	[V]	568
W1-T	[V]	708
U2-V2	[V]	0
V2-W2	[V]	0
W2-U2	[V]	0

THREE-PHASE PERMANENT MAGNETS SYNCHRONOUS MACHINE WITH DOUBLE STATOR

TEST BULLETIN NO. 6

NO-LOAD TEST AS A GENERATOR

Winding connection

Speed n = 1000RPM
Frequency f=50Hz

Voltage values at the various terminals

Voltage between terminals	Unit of measurement	Value
U1-U2	[V]	410
V1-V2	[V]	410
W1-W2	[V]	410
U1-V1	[V]	708
V1-W1	[V]	708
W1-U1	[V]	708
R-S	[V]	250
S-T	[V]	250
T-R	[V]	250
U1-R	[V]	565
U1-S	[V]	708
U1-T	[V]	466
V1-R	[V]	250
V1-S	[V]	0
V1-T	[V]	250
W1-R	[V]	468
W1-S	[V]	708
W1-T	[V]	678
U2-V2	[V]	0
V2-W2	[V]	0
W2-U2	[V]	0

THREE-PHASE PERMANENT MAGNETS SYNCHRONOUS MACHINE WITH DOUBLE STATOR

TEST BULLETIN NO. 7

NO-LOAD TEST AS A GENERATOR

Winding connection

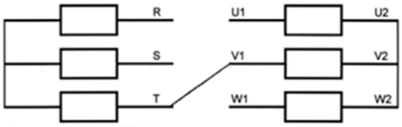

Speed n = 1000RPM
Frequency f=50Hz

Voltage values at the various terminals

Voltage between terminals	Unit of measurement	Value
U1-U2	[V]	410
V1-V2	[V]	410
W1-W2	[V]	410
U1-V1	[V]	708
V1-W1	[V]	708
W1-U1	[V]	708
R-S	[V]	250
S-T	[V]	250
T-R	[V]	250
U1-R	[V]	816
U1-S	[V]	948
U1-T	[V]	708
V1-R	[V]	250
V1-S	[V]	250
V1-T	[V]	0
W1-R	[V]	568
W1-S	[V]	816
W1-T	[V]	678
U2-V2	[V]	0
V2-W2	[V]	0
W2-U2	[V]	0

THREE-PHASE PERMANENT MAGNETS SYNCHRONOUS MACHINE WITH DOUBLE STATOR

TEST BULLETIN NO. 8

NO-LOAD TEST AS A GENERATOR

Winding connection

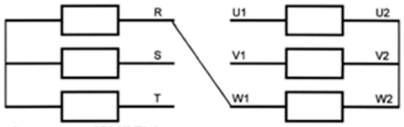

Speed n = 1000RPM
Frequency f=50Hz

Voltage values at the various terminals

Voltage between terminals	Unit of measurement	Value
U1-U2	[V]	410
V1-V2	[V]	410
W1-W2	[V]	410
U1-V1	[V]	708
V1-W1	[V]	708
W1-U1	[V]	708
R-S	[V]	250
S-T	[V]	250
T-R	[V]	250
U1-R	[V]	708
U1-S	[V]	675
U1-T	[V]	468
V1-R	[V]	708
V1-S	[V]	468
V1-T	[V]	565
W1-R	[V]	0
W1-S	[V]	250
W1-T	[V]	250
U2-V2	[V]	0
V2-W2	[V]	0
W2-U2	[V]	0

© 2025 by the author(s). Distributed under a Creative Commons CC BY license.

Preprints.org (www.preprints.org) | NOT PEER-REVIEWED | Posted: 4 August 2025 doi:10.20944/preprints202508.0088.v1

THREE-PHASE PERMANENT MAGNETS SYNCHRONOUS MACHINE WITH DOUBLE STATOR

TEST BULLETIN NO. 9

NO-LOAD TEST AS A GENERATOR

Winding connection

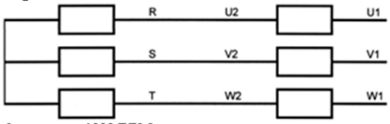

Speed n = 1000 RPM

Frequency f = 50 Hz

Voltage values at the various terminals

Voltage between terminals	Unit of measurement	Value
U1-U2	[V]	410
V1-V2	[V]	410
W1-W2	[V]	410
U1-V1	[V]	892
V1-W1	[V]	812
W1-U1	[V]	465
R-S	[V]	250
S-T	[V]	250
T-R	[V]	250
U1-R	[V]	410
U1-S	[V]	410
U1-T	[V]	410
V1-R	[V]	
V1-S	[V]	410
V1-T	[V]	
W1-R	[V]	
W1-S	[V]	
W1-T	[V]	410
U2-V2	[V]	250
V2-W2	[V]	250
W2-U2	[V]	250

THREE-PHASE PERMANENT MAGNETS SYNCHRONOUS MACHINE WITH DOUBLE STATOR

TEST BULLETIN NO. 10

TEST OPERATION AS A GENERATOR ON LOAD

Parameters	Unit of measurement	Value			
U ab	[V]	960	944	932	640
U bc	[V]	960	944	932	648
U ca	[V]	960	944	932	640
U med	[V]	960	944	932	642.6667
I a	[A]	0	1.15	2.1	3.16
I b	[A]	0	1.15	2.1	3.22
I c	[A]	0	1.15	2.1	3.18
I med	[A]	0	1.15	2.1	3.186667
f	[Hz]	50	50	50	50
cos φ	-	1	1	1	1
P	[W]	0	1880	3390	3542

External characteristic U = f (I)

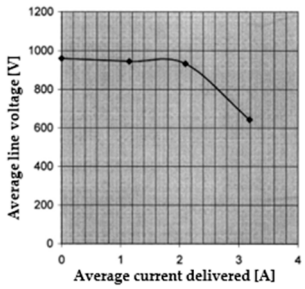

THREE-PHASE PERMANENT MAGNETS SYNCHRONOUS MACHINE WITH DOUBLE STATOR

TEST BULLETIN NO. 11

HEATING TEST IN GENERATOR MODE

Winding connection

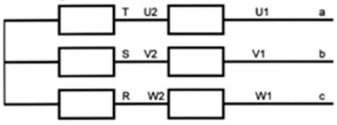

Resistive load

Service load S2-30 min

MEASURED PARAMETERS

Parameters	Unit of measurement	Value						
U ab	[V]	937	937	936	935	934	933	932
U bc	[V]	937	937	936	935	934	933	932
U ca	[V]	937	937	936	935	934	933	932
U med	[V]	937	937	936	935	934	933	932
I a	[A]	2.12	2.12	2.11	2.107	2.105	2.102	2.102
I b	[A]	2.06	2.06	2.06	2.06	2.054	2.052	2.05
I c	[A]	2.16	2.16	2.16	2.157	2.155	2.152	2.15
I med	[A]	2.113333	2.113333	2.11	2.108	2.104667	2.102	2.100667
f	[Hz]	50	50	50	50	50	50	50
cos φ	-	1	1	1	1	1	1	1
P	[W]	3429.795	3429.795	3420.731	3413.838	3404.794	3396.839	3391.046
Time	[s]	0	5	10	15	20	25	30

THREE-PHASE PERMANENT MAGNETS SYNCHRONOUS MACHINE WITH DOUBLE STATOR

TEST BULLETIN NO. 12

HEATING TEST IN GENERATOR MODE

Heating test results

Service load	S2-30 min	
Voltage	932	[V]
Current	2.1	[A]
Power	3391	[W]
Frequency	50	[Hz]

Determining the heating values of the outer winding

Quantities for determining heating							
	U cc	1.674	1.67	1.667	1.666	1.665	[V]
	I cc	1.1	1.1	1.1	1.1	1.1	[A]
	Resistance	1.521818	1.518182	1.515455	1.514545	1.513636	[Ω]
Winding heating		15.54325	14.8944	14.40776	14.24555	14.08334	[°C]
Time since shutdown		50	76	115	130	145	[s]

Winding interruption characteristic after load interruption

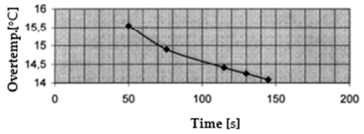

Determination of internal winding heating values

Quantities for determining heating							
	U cc	1.25	1.239	1.237	1.235	1.234	[V]
	I cc	1.103	1.103	1.103	1.103	1.103	[A]
	Resistance	1.133273	1.1233	1.121487	1.119674	1.118767	[Ω]
Winding heating		17.0519	14.64904	14.21216	13.77528	13.55684	[°C]
Time since shutdown		65	105	120	138	155	[s]

Winding interruption characteristic after load interruption

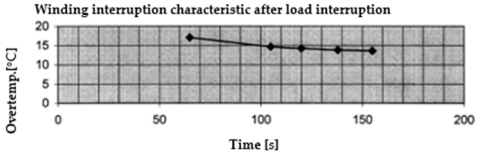

© 2025 by the author(s). Distributed under a Creative Commons CC BY license.

Preprints.org (www.preprints.org) | NOT PEER-REVIEWED | Posted: 4 August 2025 doi:10.20944/preprints202508.0088.v1

THREE-PHASE PERMANENT MAGNETS SYNCHRONOUS MACHINE WITH DOUBLE STATOR

TEST BULLETIN NO. 13

HEATING TEST IN GENERATOR MODE

Winding connection

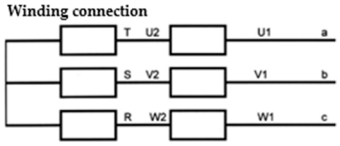

Resistive load

Service load S2-105 min

MEASURED PARAMETERS

Parameters	Unit of measurement	Value						
U ab	[V]	630	629	628	627	626	625	624
U bc	[V]	638.0769	637.0641	636.0513	635.0385	634.0256	633.0128	632
U ca	[V]	634.0385	633.0321	632.0256	631.0192	630.0128	629.0064	628
U med	[V]	634.0385	633.0321	632.0256	631.0192	630.0128	629.0064	628
I a	[A]	3.210577	3.205481	3.200385	3.195288	3.190192	3.185096	3.18
I b	[A]	3.170192	3.16516	3.160128	3.155096	3.150064	3.145032	3.14
I c	[A]	3.190385	3.185321	3.180256	3.175192	3.170128	3.165064	3.16
I med	[A]	3.190385	3.185321	3.180256	3.175192	3.170128	3.165064	3.16
f	[Hz]	50	50	50	50	50	50	50
cos φ	-	1	1	1	1	1	1	1
P	[W]	3503.638	3492.525	3481.428	3470.35	3459.289	3448.246	3437.22
Time	[s]	15	30	45	60	75	90	105

THREE-PHASE PERMANENT MAGNETS SYNCHRONOUS MACHINE WITH DOUBLE STATOR

TEST BULLETIN NO. 14

HEATING TEST IN GENERATOR MODE

Heating test results

Service load	S2-105 min	
Voltage	628	[V]
Current	3.16	[A]
Power	3437	[W]
Frequency	50	[Hz]

Determining the heating values of the outer winding

Quantities for determining heating							
	U cc	1.798	1.794	1.792	1.79	1.787	[V]
	I cc	1.1	1.1	1.1	1.1	1.1	[A]
	Resistance	1.634545	1.630909	1.629091	1.627273	1.624545	[Ω]
Winding heating		35.65756	35.00872	34.68429	34.35987	33.87323	[°C]
Time since shutdown		36	55	70	80	105	[s]

Winding interruption characteristic after load interruption

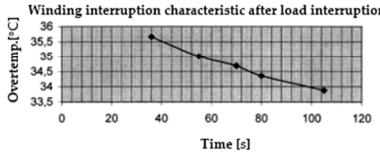

Determination of internal winding heating values

Quantities for determining heating							
	U cc	1.356	1.355	1.354	1.353	1.352	[V]
	I cc	1.1	1.1	1.1	1.1	1.1	[A]
	Resistance	1.232727	1.231818	1.230909	1.23	1.229091	[Ω]
Winding heating		41.01454	40.7955	40.57646	40.35743	40.13839	[°C]
Time since shutdown		47	62	75	95	115	[s]

Winding interruption characteristic after load interruption

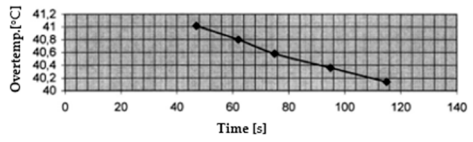

THREE-PHASE PERMANENT MAGNETS SYNCHRONOUS MACHINE WITH DOUBLE STATOR

TEST BULLETIN NO. 15

HEATING TEST IN GENERATOR MODE

Winding connection

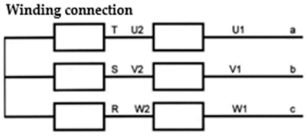

Resistive load

Service load S1- continuously

MEASURED PARAMETERS

Parameters	Unit of measurement	Value						
U ab	[V]	622	621	620	619	618	617	616
U bc	[V]	630.0779	629.0649	628.0519	627.039	626.026	625.013	624
U ca	[V]	624.0195	623.0162	622.013	621.0097	620.0065	619.0032	618
U med	[V]	625.3658	624.3604	623.355	622.3496	621.3442	620.3387	619.3333
I a	[A]	3.079708	3.074756	3.069805	3.064854	3.059903	3.054951	3.05
I b	[A]	3.120097	3.115081	3.110065	3.105049	3.100032	3.095016	3.09
I c	[A]	3.190779	3.185649	3.180519	3.17539	3.17026	3.16513	3.16
I med	[A]	3.130195	3.125162	3.12013	3.115097	3.110065	3.105032	3.1
f	[Hz]	50	50	50	50	50	50	50
cos φ	-	1	1	1	1	1	1	1
P	[W]	3390.519	3379.625	3368.75	3357.891	3347.051	3336.228	3325.422
Time	[s]	30	60	90	120	150	180	210

THREE-PHASE PERMANENT MAGNETS SYNCHRONOUS MACHINE WITH DOUBLE STATOR

TEST BULLETIN NO. 16

HEATING TEST IN GENERATOR MODE

Heating test results

Service load	S1- continuously	
Voltage	619	[V]
Current	3.1	[A]
Power	3325	[W]
Frequency	50	[Hz]

Determining the heating values of the outer winding

Quantities for determining heating							
	U cc	1.868	1.864	1.86	1.857	1.855	[V]
	I cc	1.1	1.1	1.1	1.1	1.1	[A]
	Resistance	1.698182	1.694545	1.690909	1.688182	1.686364	[Ω]
Winding heating		47.01242	46.36357	45.71472	45.22808	44.90366	[°C]
Time since shutdown		30	50	70	90	110	[s]

Winding interruption characteristic after load interruption

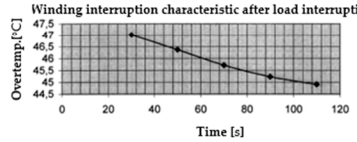

Determination of internal winding heating values

Quantities for determining heating							
	U cc	1.428	1.4265	1.424	1.422	1.421	[V]
	I cc	1.1	1.1	1.099	1.098	1.098	[A]
	Resistance	1.298182	1.296818	1.295723	1.295082	1.295082	[Ω]
Winding heating		56.78522	56.45666	56.19288	56.03834	55.8189	[°C]
Time since shutdown		40	60	80	100	120	[s]

Winding interruption characteristic after load interruption

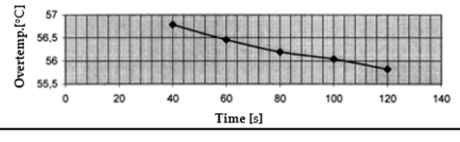

4. Conclusions

As we have shown throughout this presentation, the proposed structure is equivalent to two classical permanent magnet synchronous machines, electrically connected in series and coupled on

© 2025 by the author(s). Distributed under a Creative Commons CC BY license.

Preprints.org (www.preprints.org) | NOT PEER-REVIEWED | Posted: 4 August 2025 doi:10.20944/preprints202508.0088.v1

the same shaft. These elementary machines operate at the same autopilot angle, but the power factors and internal angles are different. Overall, however, the structure with the two stators behaves like a classical permanent magnet synchronous machine.

The two elementary machines can be separated by a cylindrical sectioning at the rotor level and studied separately. The analytical calculation model leads to slightly superior results to those obtained by numerical simulation (within the range of 5%).

By using a double surface of interaction of the rotor with the two stators, the electromagnetic torque and the active power are significantly superior to a classic machine with the same volume of active materials, even going as far as doubling the respective sizes. In addition, the cantilever rotor has a reduced inertia and is more robust in terms of mechanical construction, only the fixing of the magnets posing some technological problems.

The synchronous variant makes better use of the new structure, the reunion of the two machines being possible without modifying their transverse geometry. By fixing rare earth permanent magnets on both the outer and inner face of the rotor - made of solid steel pipe - significant fluxes are ensured that can be closed independently of each other. In this way, each active area of notches - air gap - permanent magnets can be used optimally.

In the synchronous version, the specific torques (Nm/kg of active material) increase impressively compared to synchronous motors with permanent magnets of normal construction. From a mechanical point of view, the rotor is more robust than in the asynchronous version, also benefiting from a reduced inertia.

The results of simulations using numerical methods and analytical calculations justify the conclusion that the proposed structure is of theoretical and practical interest, and the execution of a prototype with two interchangeable rotors will be able to confirm the technical and economic advantages of this solution.

Author Contributions: Conceptualization, M.-F.S. and I.B.; methodology, M.-F.S., I.B. and T.I; software M.-F.S., I.B. and T.I; validation, M.-F.S., I.B.; formal analysis, I.B. and T.I.; investigation, M.-F.S., I.B., T.I.; resources, M.-F.S.; writing—original draft preparation, M.-F.S. and I.B.; writing—review and editing, M.-F.S., I.B., T.I.; visualization, I.B. and T.I.; supervision, M.-F.S. and I.B. All authors have read and agreed to the published version of the manuscript.

Funding: This research was funded by Valahia University of Targoviste, Romania.

Data Availability Statement: Data is contained within the article.

Conflicts of Interest: The authors declare no conflicts of interest.

References

1. Heim, J.W.; Vander Wal, R.L. NdFeB Permanent Magnet Uses, Projected Growth Rates and Nd Plus Dy Demands across End-Use Sectors through 2050: A Review. *Minerals* **2023**, *13*(10), 1274.
2. Kaya, M. NdFeB Permanent Magnet Uses, An overview of NdFeB magnets recycling technologies. *Current Opinion in Green and Sustainable Chemistry* **2024**, *46*, 100884.
3. Kumari, A.; Sahu, S.K. A comprehensive review on recycling of critical raw materials from spent neodymium iron boron (NdFeB) magnet. *Separation and Purification Technology* **2023**, *317*, 123527.
4. Crozier-Bioud, T.; Momeni, V.; Gonzalez-Gutierrez, J.; Kukla, C.; Luca, S.; Rolere, S. Current challenges in NdFeB permanent magnets manufacturing by Powder Injection Molding (PIM): A review. *Materials Today Physics* **2023**, *34*, 101082.
5. Kaya, E.E.; Kaya, O.; Stopic, S.; Gürmen, S.; and Friedrich, B. NdFeB Magnets Recycling Process: An Alternative Method to Produce Mixed Rare Earth Oxide from Scrap NdFeB Magnets. *Metals* **2021**, *11*(5), 716.
6. Lee, J.I.; Kim, Y.C.; Jang-Young Choi, J.Y.; and Cho, H.W. Analysis of Electromagnetic–Mechanical Characteristics according to Shaft Materials of Permanent Magnet Synchronous Motor. *Energies* **2022**, *15*(21), 8046.

© 2025 by the author(s). Distributed under a Creative Commons CC BY license.

Preprints.org (www.preprints.org) | NOT PEER-REVIEWED | Posted: 4 August 2025 doi:10.20944/preprints202508.0088.v1

7. Kumar, R.; Murmu, R. Performance Analysis of Permanent Magnet Synchronous Motor. *International Journal of Engineering Research & Technology (IJERT)* **2020**, *8*(16), 16026.
8. Nagamuneendra, P.; Haritha, K. A Review on Design and Control of Permanent Magnet Synchronous Motor. *International Journal of Advance Research and Innovative Ideas in Education (IJARIIE)* **2024**, *10*(6), 25460.
9. Shangguan, X.; Xie, Y.; Wang, X.; Wang, Q. Characteristic Analysis and Optimization Design of Permanent Magnet Synchronous Motor with New Rotor Structure. *International Core Journal of Engineering* **2025**, *11*(6), 0026.
10. Shen, Q.; Zhou, Z.; Li, S.; Liao, X.; Wang, T.; He, X.; Zhang, J. Design and Analysis of the High-Speed Permanent Magnet Motors: A Review on the State of the Art. *Machines* **2022**, *10*, 549.
11. Tun, M.Z.; Swe, P.L. Power Factor Correction with Synchronous Motor for Rice Mill. *International Journal of Scientific Engineering and Technology Research (IJSETR)* **2014**, *03*(07), 1150-1155.
12. Ullah, A.; Pan, J.; Safeer Ullah, S.; Zhang, Z. Robust Speed Control of Permanent Magnet Synchronous Motor Drive System Using Sliding-Mode Disturbance Observer-Based Variable-Gain Fractional-Order Super-Twisting Sliding-Mode Control. *Fractal Fract.* **2024**, *8*(7), 368.
13. Khanh, P.Q.; Truong, V.A.; Huy-Anh, H.P. Extended Permanent Magnet Synchronous Motors Speed Range Based on the Active and Reactive Power Control of Inverters. *Energies* **2021**, *14*(12), 3549.
14. Joshi, Y.; Parikh, K. Permanent Magnet Synchronous Motor Drives Control Technology. *International Journal of Engineering Research & Technology (IJERT)* **2014**, *2*(10), 10054.
15. Abdelaziz, I.M.; Mohamed, Y.S.; Zaki-Diab, A.A.; Shehata, E.G. High-Performance Control of Permanent Magnet Synchronous Motor under Different Modes of Operation. *Journal of Advanced Engineering Trends (JAET)* **2023**, *42*(2), 245-254.
16. Vannini, A.; Simonelli, C.; Marfoli, A.; Papini, L.; Bolognesi, P.; Gerada C. Modelling, Analysis, and Design of a Line-Start Permanent Magnet Synchronous Motor. *2022 International Conference on Electrical Machines (ICEM)* **2022**, DOI: 10.1109/ICEM51905.2022.9910937.
17. Sarac, V.; Minovski, D.; Janiga, P. Parametric Analysis for Performance Optimization of Line-Start Synchronous Motor with Interior Asymmetric Permanent Magnet Array Rotor Topology. *Electronics* **2022**, *11*(4), 531.
18. Zöhra, B.; Akar, M.; Eker, M. Design of a Novel Line Start Synchronous Motor Rotor. *Electronics* **2019**, *8*, 25.
19. Sethupathi, P.; Senthilnathan, N. Comparative analysis of line-start permanent magnet synchronous motor and squirrel cage induction motor under customary power quality indices. *Electrical Engineering* **2020**, *102*(3), 1339.
20. Muteba, M. Dual Stator Dual Rotor Interior Permanent Magnet Synchronous Motor for Hybrid Electric Vehicles. *2020 IEEE Transportation Electrification Conference & Expo (ITEC)*, ISSN: 2377-5483, 23-26 June **2020**.
21. Li, C.; Guo, X.; Fu, J.; Fu, W.; Liu, Y. Design and Analysis of a Novel Double-Stator Double-Rotor Motor Drive System for In-Wheel Direct Drive of Electric Vehicles. *Machines* **2022**, *10*(1), 27.
22. Diao, T. Study on Dual-Rotor Permanent Magnet Induction Motor and Performance. *The Open Electrical & Electronic Engineering Journal* **2015**, *9*(1), 584-590.
23. Flah, A.; Khan, I.A.; Agarwal, A.; Sbita, L.; Simoes, M.G. Field-oriented control strategy for double-stator single-rotor and double-rotor single-stator permanent magnet machine: Design and operation. *Computers & Electrical Engineering*, Volume 90, March **2021**, 106953
24. Wu, J.; Hu, Y.; Zhang, B.; Feng, G.; Liu, Z., M. Comparison and analysis of different rotor structures of double-stator permanent magnet synchronous motor. *IET Electric Power Applications*, June **2022**, *16*(6), 685-700.
25. Jeong, K.I.; Heidari, R; Kang, D.H.; Ahn, T.J.; Park, G.S.; Ahn, J.W.; Lukman, G.F. Electromagnetic Characteristics of Dual-Air-Gap Surface Permanent Magnet Synchronous Motor. *Machines* **2023**, *11*, 717.
26. Zhu, M.; Wu, L.; Liu, D.; Yiming Shen, Y.; Li, R.; Wen, H. Comparative Study of Dual-Stator Permanent Magnet Machines with Different PM Arrangements and Rotor Topologies for Aviation Electric Propulsion. *Machines* **2025**, *13*(4), 273.

© 2025 by the author(s). Distributed under a Creative Commons CC BY license.

Preprints.org (www.preprints.org) | NOT PEER-REVIEWED | Posted: 4 August 2025 doi:10.20944/preprints202508.0088.v1

27. Ran, Z.; Zi-Qiang Zhu, Z.Q.; Liang, D. Comparative Study of Dual-Rotor Permanent Magnet Machines with Series and Parallel Magnetic Circuits. *World Electr. Veh. J.* **2025**, *16*, 12.
28. Stan, M.F.; Bancuta, I.; Virjoghe, E.O.; Husu, A.G.; Cobianu, C. Unconventional Structures of Asynchronous Motors with Two Stators and Single-Rotor Radial Air Gaps in the Context of Their Applicability Assessment. *Energies* **2024**, *17*(24), 6237.
29. Hao, W.; Zhang, G.; Liu, W.; Liu, H.; Wang, Y. Methods for Reducing Cogging Force in Permanent Magnet Machines: A Review. *Energies* **2023**, *16*(1), 422.
30. Yan, D.; Yan, Y.; Cheng, Y.; Guo, L.; Shi, T. Research on cogging torque reduction method for permanent magnet synchronous motor accounting for the magnetic pole edge effect. *IET Electric Power Applications* **2024**, *18*(1), 64–75, 12367.
31. Anuja, T.A.; Arun Noyal Doss, M. Reduction of Cogging Torque in Surface Mounted Permanent Magnet Brushless DC Motor by Adapting Rotor Magnetic Displacement. *Energies* **2021**, *14*, 2861.
32. Caruso, M.; Di Tommaso, A.O.; Miceli, R.; Viola, F. A Cogging Torque Minimization Procedure for Interior Permanent Magnet Synchronous Motors Based on a Progressive Modification of the Rotor Lamination Geometry. *Energies* **2022**, *15*, 4956.

Disclaimer/Publisher's Note: The statements, opinions and data contained in all publications are solely those of the individual author(s) and contributor(s) and not of MDPI and/or the editor(s). MDPI and/or the editor(s) disclaim responsibility for any injury to people or property resulting from any ideas, methods, instructions or products referred to in the content.

© 2025 by the author(s). Distributed under a Creative Commons CC BY license.